

Constraints for Jaccard index-based rotational symmetry focus position in binary images

N.A. Lomov¹, O.S. Seredin¹, D.V. Liakhov¹, O.A. Kushnir¹

¹Tula State University, 300012, Tula, Russia, Lenin Ave. 92

Abstract

This study proposes analytical estimate for the size of a binary raster figure region which is guaranteed to contain the rotational symmetry focus. Focus here is the point a maximum Jaccard index between initial figure and rotated one. The size of the region is determined by the lower estimate of the intersection area during the rotation of the approximating primitives, considering the sizes of the inner and outer parts of the figure relative to the primitive. The smallest circumscribed circle or ellipse and sets of concentric circles and ellipses produced by the principal component analysis were used as the approximating figure. To verify the hypothesis that the size of the region is insignificant compared to the area of the figure, we numerically simulated the proposed method with test image datasets.

Keywords: central symmetry, rotational symmetry, symmetry focus, Jaccard index.

Citation: Lomov NA, Seredin OS, Liakhov DV, Kushnir OA. Constraints for Jaccard index-based rotational symmetry focus position in binary images. *Computer Optics* 2023; 47(6): 948-957. DOI: 10.18287/2412-6179-CO-1357.

Acknowledgments: This study is supported by the Russian Science Foundation, grant No. 22-21-00575, <https://rscf.ru/project/22-21-00575/>.

Introduction

Rotational symmetry detection is not a popular problem in computer vision research, although it was studied in [1–4]. One way to detect the central point (focus) and determine the degree of symmetry is by representing the figure boundary with a special code with subsequent analysis of the cyclic structure in the resulting sequence. The method presented in the most recent paper [5] demonstrates good detection in perfectly symmetric figures, but the study does not cover the approximate symmetry detection or the corresponding metrics.

The study [6] proposes to use the intuitive Jaccard index (the ratio of the intersection over the union) for the original

and rotated figures (see Fig. 1) as a symmetry measure to find the most suitable position of the central symmetry focus in binary raster images [7]. In this study the focus is understood as the point that maximizes the symmetry function describing dependence of the symmetry measure on the rotation point. It is assumed that the solutions found can be verified with the basic exhaustive brute-force procedure applied to all the image pixels in some neighborhood of interest. The optimal symmetry measure value estimated for real-life images (e.g., scanned plant leaves, binarized objects of interest in digital photos) rarely reaches 1. In [6] authors call images with a symmetry measure close to 1 as having rotational “quasi-symmetry”. We mean this fact, but we will not use this term in this paper.

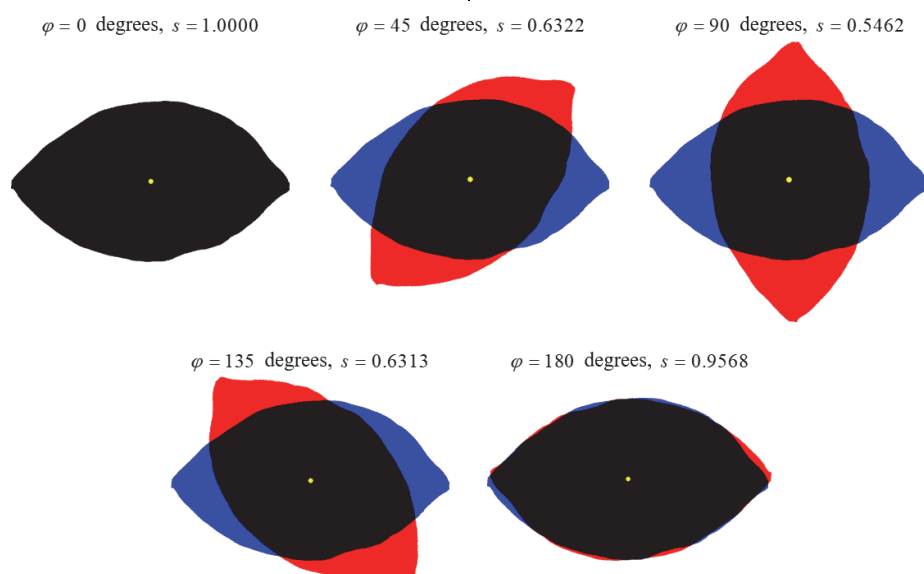


Fig. 1. Example: the symmetry function value s as the figure is rotated around a point. The original figure is blue, the rotated figure is red, and their intersection is black

For each point in the region of interest, we can plot the Jaccard index $J(\varphi)$ vs. angle curve 0 (see Fig. 2, 3) with a certain discretization rate at the angles. By analyzing such curves at various points of the image we can locate the rotational symmetry focus and estimate the degree (order) of symmetry. Note that if only central symmetry (degree 2) is considered, or there are assumptions about the degree k of the figure's rotational symmetry, we can use only $\lfloor k/2 \rfloor$ discrete angles in $2\pi/k$ increments. For example, for a figure with degree 7 it is sufficient to consider only three rotations by $2\pi/7$, $4\pi/7$, and $6\pi/7$ angles. This assumption significantly reduces the computational cost: it is enough to estimate the degree of symmetry for several discrete angles. Still, to find the focus (the point with the max Jaccard index representing the symmetry between the original and the rotated figures) we should either look through the points of some region of a given size or use the quick search procedure which skips some points.

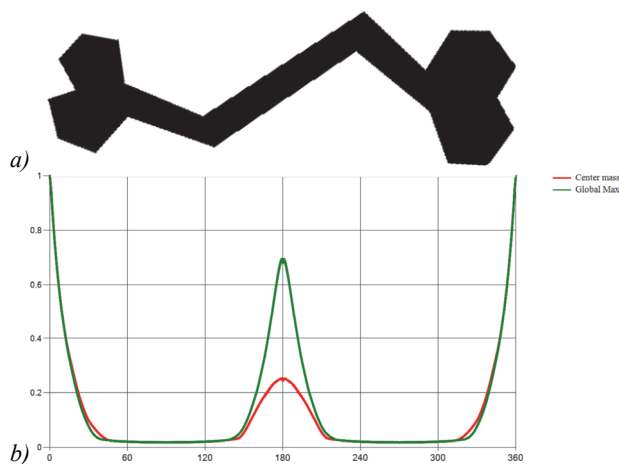


Fig. 2. a) Figure in the binary image. b) Jaccard index values as the figure rotates around the center of mass (red curve) and the rotational symmetry focus (green curve)

The paper [6] proposes such a quick procedure based on the quadratic approximation of the symmetry function. However, the size of the neighborhood is set arbitrarily. Particularly, the points within a circle with the radius r and center coinciding with the center of mass of the binary raster image are considered the neighborhood points. The size of the neighborhood region is defined as $r = \lambda R$, where R is the radius of the circle circumscribed around the figure, or the distance from the center of mass to the farthest point of the figure, $\lambda \in (0..1]$ is the value specifying the size of the search domain (see Fig. 3). For the numerical experiments, this value was set to 0.1 or 0.15 without any theoretical explanation. Obviously, the greater the λ value, the more points are to be evaluated.

The method proposed in [8] is also reduced to the detection of the region of interest which contains the rotational symmetry focus. For this, the Radon transform of the binary figure is analyzed. It is shown that the upper estimates on the Jaccard index can be found by comparing the transform curves for the angles that are shifted by

the angle of rotation apart. As a result, the Jaccard index is calculated only for the focus positions with the upper estimate better than that of the initial approximation.

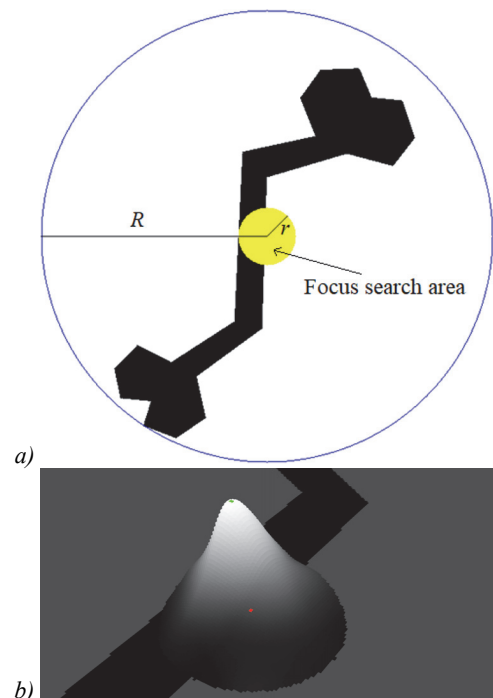


Fig. 3. a) The central symmetry focus search domain around the center of mass $r = \lambda R$, $\lambda = 0.15$. b) The central symmetry function value in the neighborhood of the center of mass (red dot). The green dot marks the maximum value

In this study, we showed how the size of the circle or ellipse neighborhood containing the rotational symmetry focus can be obtained analytically. We also assume that the size is small relative to the size of the figure. To confirm this hypothesis, we estimated the performance of the proposed procedure as the ratio of the detected region size to the size of the circumscribed circle of the figure.

In general, approximation rather than the precise calculation of the geometric properties of a figure by statistical analysis of its coordinates or their projections can indeed be found in computational geometry and computer vision problems. For example, the paper [9] gives approximate estimates of the size of the bounding rectangular parallelepiped with its sides being parallel to the axes of the principal components relative to the min size bounding parallelepiped. The study [10] offers approximate estimates for the distance between convex polyhedra using their circumscribed ellipsoids.

1. Neighborhood definition

1.1. The general principle of determining the neighborhood containing the focus of the central symmetry

We will consider the basic case of degree 2 rotational symmetry (central symmetry). It is reduced to the comparison of the original image and the image rotated by 180 degrees.

The general approach to estimating the shape and size of the region which contains the optimal central sym-

metry is as follows. Let the figure A , for which we detect the focus position, be inscribed in the figure B . When rotated around the optimal focus by the same angle (and after any bijective transform in general), the A' and B' figures are generated, respectively. Then the figure $A' \cap A$ is inscribed into the figure $B' \cap B$. As we know the lower estimate of $|A' \cap A|$, we can use it as the estimate from below for $|B' \cap B|$, reducing the rotation parameters to the values for which this estimate is valid (Fig. 4).

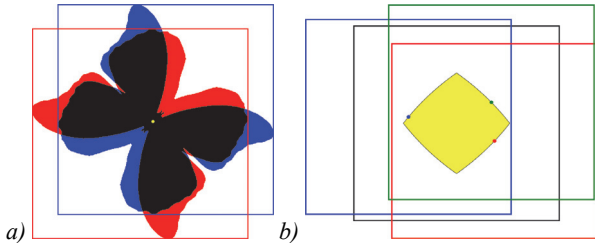


Fig. 4. Illustration of upper bound of intersection estimation using enveloping figure. a) Original figure (blue and black), rotated figure (red and black), and their enveloping rectangles. b) The possible position of rotation point (the boundary of the yellow figure) with fixed intersection area between rotated (colored) and initial (black) rectangles

1.2. Circumscribed circle

As the circle is “isomorphous” in all directions, it is convenient to use circles circumscribed around the figures. Then $|B' \cap B|$ for the fixed circle radius r depends only on the distance d from circle center to the pivot point. At $d \leq r$, the intersection of the circles is a lens-shaped region consisting of two equally-sized circular segments (Fig. 5a). At $d > r$, the intersection is empty.

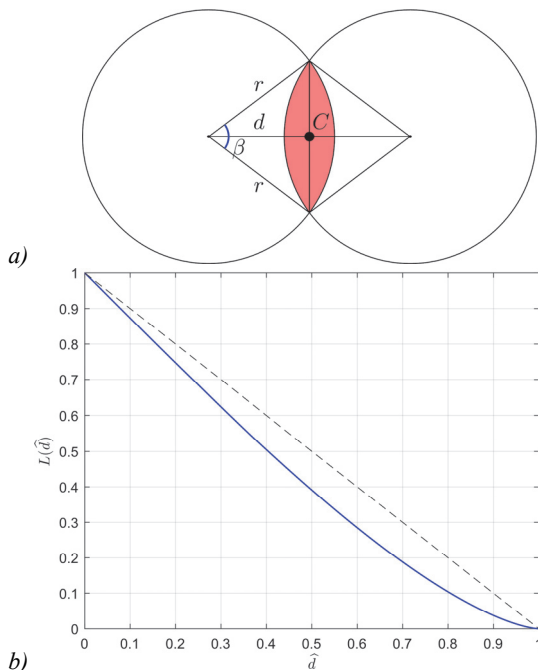


Fig. 5. a) The intersection of the circles is symmetrical about the point C . b) The intersection area share for the circle area vs. distance to the pivot point is expressed in fractions of the radius

Segments' angular value is $2\arccos(d/r)$. Respectively, the area of the lens-shaped region is:

$$L(d,r) = \begin{cases} r^2 \left(2\arccos \frac{d}{r} - \sin \left(2\arccos \frac{d}{r} \right) \right) & d \leq r, \\ 0 & d > r. \end{cases} \quad (1)$$

To remove the second argument, we will represent d not as an absolute value but as a fraction of the radius $\hat{d} = d/r$. The area is also normalized to the total area of the circle πr^2 (to obtain a fraction of the area):

$$L(\hat{d}) = \begin{cases} \frac{2\arccos \hat{d} - \sin(2\arccos \hat{d})}{\pi} & \hat{d} \leq 1, \\ 0 & \hat{d} > 1. \end{cases} \quad (2)$$

Fig. 5b shows the function plot. It is decreasing in \hat{d} over the $[0,1]$ segment, so for $|A' \cap A| = s$ the following statement is true: if the fraction of the intersection area is not less than $\hat{s} = s/\pi r^2$ of the area of the circumscribed circle B with the radius r , the optimal pivot point is no farther than $rL^{-1}(\hat{s})$ from the center B , since only for such values the lens-shaped region sufficient to contain the entire intersection region is at its minimum. Note: for $\hat{s} \leq 0$, $L^{-1}(\hat{s})$ is assumed equal to $+\infty$.

To estimate $|A' \cap A|$ from below, it would be natural to use some approximation of the optimal pivot point, e.g., the center of mass of the figure A . The circumscribed circle should have the smallest radius possible (its center does not have to be at the center of mass) to increase the fraction of the area and diminish the multiplier at $L^{-1}(\hat{s})$. The result is shown in Fig. 6. It leads to the conclusion that the estimate obtained so far is very imprecise.

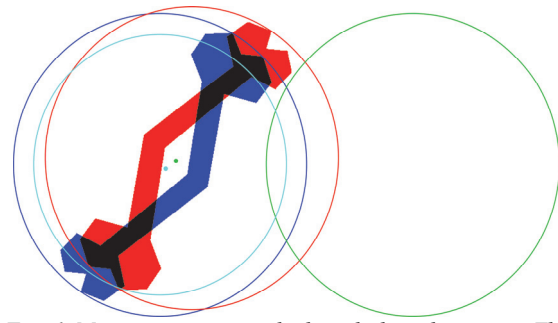


Fig. 6. Minimum circumscribed circle-based estimate. The original figure is blue, the symmetric figure relative to the center of mass is red, and their intersection region is black. The circumscribed circles of figures have the same colors. The green circle is one of the circles which intersect the original circle producing a lens-shaped region with a size equal to the size of the intersection region. The turquoise circle is the neighborhood containing the optimal pivot point. The center of mass is the green dot. The turquoise point is the optimal focus

1.3. Circumscribed ellipse

An obvious disadvantage of the above method is the overestimation of elongated figures. The fraction of their area relative to the area of the circumscribed circle is low, which leads to a low \hat{s} and a higher distance from the possible pivot point position to the center of the circle.

We will use an ellipse as the circumscribed figure. The ellipse equation is:

$$(\mathbf{p} - \mathbf{q})^T \mathbf{M}^{-1} (\mathbf{p} - \mathbf{q}) = r^2, \quad (3)$$

where \mathbf{M} is a positive definite matrix, \mathbf{q} is a center of ellipse. For a central symmetry with the center at \mathbf{c} the point \mathbf{p}' such that \mathbf{c} is the midpoint of the segment \mathbf{pp}' (in other words, $\mathbf{p}' = 2\mathbf{c} - \mathbf{p}$) is symmetric to the point \mathbf{p} . Then for center of symmetry $\mathbf{q}' = 2\mathbf{c} - \mathbf{q}$

$$\begin{aligned} (\mathbf{p}' - \mathbf{q}')^T \mathbf{M}^{-1} (\mathbf{p}' - \mathbf{q}') &= \\ ((2\mathbf{c} - \mathbf{p}) - (2\mathbf{c} - \mathbf{q}))^T \mathbf{M}^{-1} ((2\mathbf{c} - \mathbf{p}) - (2\mathbf{c} - \mathbf{q})) &= \\ = (\mathbf{q} - \mathbf{p})^T \mathbf{M}^{-1} (\mathbf{q} - \mathbf{p}) = (\mathbf{p} - \mathbf{q})^T \mathbf{M}^{-1} (\mathbf{p} - \mathbf{q}) &= r^2, \end{aligned} \quad (4)$$

that is, \mathbf{p}' belongs to the ellipse with the center at \mathbf{q}' produced by shifting the original one. We will apply a linear transform of coordinates using the matrix. The transform maps point $\mathbf{p}^* = \mathbf{M}^{-1/2} \mathbf{p}$ to point \mathbf{p} . Therefore, $\mathbf{p} = \mathbf{M}^{1/2} \mathbf{p}^*$. After the transform, the points of the original ellipse are defined by the equation

$$\begin{aligned} (\mathbf{p} - \mathbf{q})^T \mathbf{M}^{-1} (\mathbf{p} - \mathbf{q}) &= \\ (\mathbf{p}^* - \mathbf{q}^*)^T (\mathbf{M}^{1/2})^T \mathbf{M}^{-1} \mathbf{M}^{1/2} (\mathbf{p}^* - \mathbf{q}^*) &= \\ (\mathbf{p}^* - \mathbf{q}^*)^T (\mathbf{p}^* - \mathbf{q}^*) &= r^2, \end{aligned} \quad (5)$$

that is the equation of a circle with the radius r . Note that the transform increases the areas by a factor of $\det \mathbf{M}^{-1/2}$ (or decreases by a factor of $\det \mathbf{M}^{1/2} = \sqrt{\det \mathbf{M}}$). Then, the area of the original ellipse is $\sqrt{\det \mathbf{M}}$ times of the circle area and is equal to $\pi r^2 \sqrt{\det \mathbf{M}}$. Since the directions of the major axes of the original and rotated ellipses coincide, after the transform, both ellipses turn into circles. We can assume that the problem is reduced to the previous one (Fig. 7b).

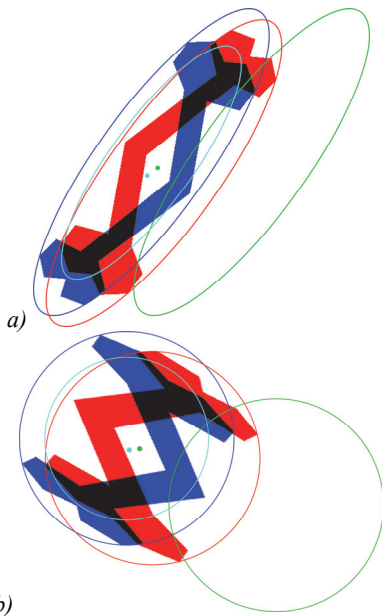


Fig. 7. Minimum circumscribed ellipse-based estimate. a) Constructions in the original space. b) Constructions in the "expanding" space, reducing the problem to the case of circles. Refer to Fig. 6 for the colors

Since the affine transform does not change the ratio of areas, we can again apply the rule: if the fraction of the intersection area $|A' \cap A| = s$ is not less than $\hat{s} = s / \pi r^2 \sqrt{\det \mathbf{M}}$ of the circumscribed ellipse area E defined by the equation $(\mathbf{p}' - \mathbf{q}')^T \mathbf{M}^{-1} (\mathbf{p}' - \mathbf{q}') = r^2$, the optimal pivot point is located inside a concentric figure obtained by compressing the original figure along the axes $L^{-1}(\hat{s})$ -fold, that is, the ellipse defined by the equation $(\mathbf{p}' - \mathbf{q}')^T \mathbf{M}^{-1} (\mathbf{p}' - \mathbf{q}') = (rL^{-1}(\hat{s}))^2$ (refer to Fig. 7a). Note that this estimate is certainly no worse than the first one since the circle is a special case of the ellipse. For the figure shown in Figs. 6–7 the area of the elliptic neighborhood is 45 % of the circle area.

1.4. Approximating circle/ellipse

Another disadvantage of this approach is its low resistance to noise. If we add thin protrusions or, moreover, isolated points to the figure, the size of the circumscribed circle may increase dramatically, despite that neither the area nor shape of the figure changed significantly. We need an approach that ignores such shape changes as far as possible. We will relax the requirements for the ellipse. Now the ellipse is allowed not to cover the figure completely, but to cover as much of the figure as possible while having the smallest radius possible. For the ellipse E let us suppose that a part of the figure A with the area s_{in} is inside it, and a part of the figure A with the area s_{out} is beyond it. Then $|A' \cap A|$ is the sum of the intersection region areas inside and outside the elliptical lens-shaped region, and the former does not exceed s_{in} , while the latter does not exceed s_{out} . We need to find the lower estimate of the lens-shaped region area. $s - s_{out}$ can be used as such. Then the estimate for the given ellipse is:

$$d \leq rL^{-1} \left(\frac{s - s_{out}}{\pi r^2 \sqrt{\det \mathbf{M}}} \right). \quad (6)$$

Fig. 8 shows an example of an estimate with this version of the method.

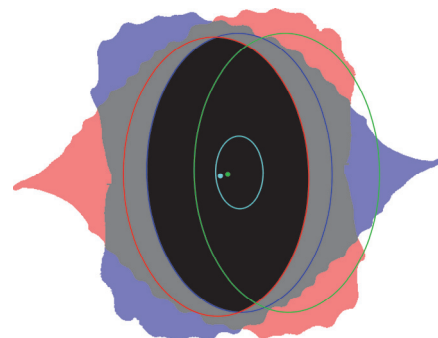


Fig. 8. Approximating ellipse-based estimate. The part of the figure outside the intersection of the ellipses is filled with pale colors. Otherwise, the colors are the same as in Figs. 6-7

1.5. Rotational symmetry of degrees greater than 2

So far, we considered central symmetry or rotational symmetry of degree 2. The solution is reduced to the comparison of the Jaccard indices of the two figures.

When analyzing a degree $k > 2$ symmetry, it is natural to make a general comparison k of the figures A_0, \dots, A_{k-1} resulting from rotations by

$$\left\{ \frac{2\pi i}{k} \right\}_{i=0}^{k-1}.$$

The study [8] proposes to average the pairwise comparison metrics using the generalized Jaccard index

$$J^{(k)}(A) = \frac{\sum_{0 \leq i < j \leq k-1} |A_i \cap A_j|}{\sum_{0 \leq i < j \leq k-1} |A_i \cup A_j|}. \quad (7)$$

As such a comparison is identical to the rotations by α and $-\alpha$, the problem can be simplified to $\lfloor k/2 \rfloor$ rotations:

$$J^{(k)}(A) = \begin{cases} \frac{\sum_{i=1}^{\lfloor \frac{k-1}{2} \rfloor} |A_0 \cap A_i|}{\sum_{i=1}^{\lfloor \frac{k-1}{2} \rfloor} |A_0 \cup A_i|}, & k \text{ is odd,} \\ \frac{\left(\sum_{i=1}^{\lfloor \frac{k-1}{2} \rfloor} 2|A_0 \cap A_i| \right) + |A_0 \cap A_{\frac{k}{2}}|}{\left(\sum_{i=1}^{\lfloor \frac{k-1}{2} \rfloor} 2|A_0 \cup A_i| \right) + |A_0 \cup A_{\frac{k}{2}}|}, & k \text{ is even.} \end{cases} \quad (8)$$

Since this value is monotonically dependent on the numerator, it is sufficient to optimize only the numerator. Let us consider the approximating circle and the result of its rotation by the angle α about a point located at the d distance from its center. The center-to-center distance for the circles is $2d \sin(\alpha/2)$. Therefore, it is identical to the central symmetry when rotating around a point located at the $d_0 = d \sin(\alpha/2)$ distance (Fig. 9a). The area of the lens-shaped intersection region is

$$L_i(\hat{d}) = \begin{cases} \frac{2 \arccos\left(\hat{d} \sin \frac{\alpha_i}{2}\right) - \sin\left(2 \arccos\left(\hat{d} \sin \frac{\alpha_i}{2}\right)\right)}{\pi}, \\ \hat{d} \leq 1 / \sin \frac{\alpha_i}{2}, \\ 0, \quad \hat{d} > 1 / \sin \frac{\alpha_i}{2}, \end{cases} \quad (9)$$

where $\hat{d} = d/r$ and $\alpha = 2\pi i/k$. Let us find the area of the lens-shaped regions using the weighted Jaccard index:

$$\tilde{L}(\hat{d}) = \begin{cases} \frac{1}{k-1} \sum_{i=1}^{\lfloor \frac{k-1}{2} \rfloor} 2L_i(\hat{d}), & k \text{ is odd,} \\ \frac{1}{k-1} \left(\left(\sum_{i=1}^{\lfloor \frac{k-1}{2} \rfloor} 2L_i(\hat{d}) \right) + L_k(\hat{d}) \right), & k \text{ is even.} \end{cases} \quad (10)$$

The functions are shown in Fig. 9b. They decrease over the segment

$$\left[0, 1 / \sin \frac{2\pi \lfloor k/2 \rfloor / k}{2} \right],$$

because it is a sum of other decreasing functions. We come to the expected conclusion: if the weighted, normal-

ized area of the lens-shaped region is not less than \hat{s} , then the pivot point is located no farther than $\tilde{L}^{-1}(\hat{s})$ from the center. Suppose the initial approximation is a point corresponding to the weighted sum (numerator $J^{(k)}(A)$) of the intersections \bar{s} , and a circle containing a part of the figure A with the area s_{in} inside and the area s_{out} outside is used as an approximating figure. Note that when rotated by any angle, a part of the figure with an area of no more than s_{out} can be intersected outside the lens-shaped region. Therefore, the weighted intersection area inside the lens-shaped region is at least

$$\bar{s} - \frac{1}{k-1} \sum_{i=1}^{\lfloor \frac{k}{2} \rfloor} (2 - [2i = k]) s_{out} = \bar{s} - s_{out}.$$

It results in the following estimate for the circle center to the pivot point distance:

$$d \leq r \tilde{L}^{-1} \left(\frac{\bar{s} - s_{out}}{\pi r^2} \right). \quad (11)$$

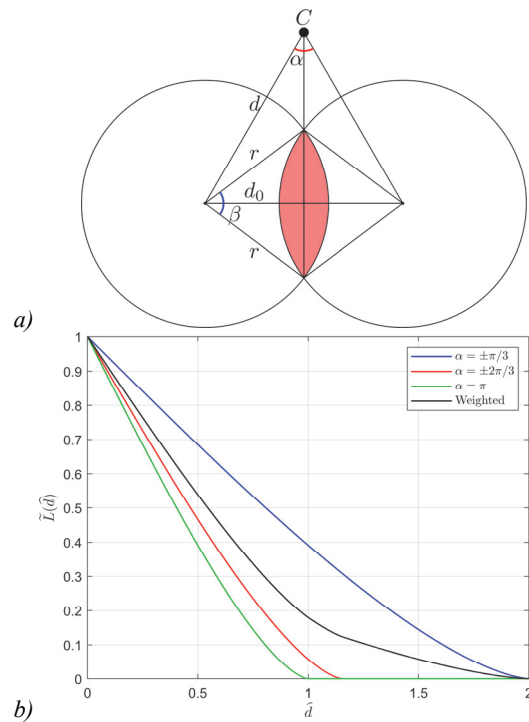


Fig. 9. a) The lens-shaped intersection region of the circles when rotating around the point C by the angle $\alpha = \pi/3$. b) Fraction of the lens-shaped region area of the circle area vs. the distance to the pivot point expressed in fractions of the radius when rotating by angles in $\pi/3$ increments

Unlike a circle, an ellipse has a degree 2 rotational symmetry and lacks any greater degree symmetries. For this reason, it does not seem reasonable to apply approximating ellipses to analyze the rotational symmetry with degrees greater than 2.

1.6. Construction of approximating figures

For our problem, the approximation is considered successful if the approximating figure has the smallest possible size while covering the original figure as much

as possible. It is natural to approximate in the regions with a high concentration of the original figure points. An obvious approach is to use approximating figures with their center at the center of mass of the figure. For ellipses, the approximating figure axes should coincide with the principal component axes. Let the figure A have the center of mass

$$\mathbf{q} = \frac{1}{|A|} \sum_{\mathbf{p} \in A} \mathbf{p}$$

and the covariance matrix $\mathbf{M} = \frac{1}{|A|} \sum_{\mathbf{p} \in A} (\mathbf{p} - \mathbf{q})(\mathbf{p} - \mathbf{q})^T$.

For degree 2 symmetry, we consider concentric ellipses defined as $(\mathbf{p}' - \mathbf{q}')^T \mathbf{M}^{-1} (\mathbf{p} - \mathbf{q}) = r^2$. The best intersection region found is again denoted by s . The "outside" area of the figure A vs. the radius of the ellipse relation is $s_{out}(r)$. We can assume that each ellipse produces a different estimate for the size of the ellipse containing the optimal focus:

$$d(r) = rL^{-1}(\hat{s}), \text{ where } \hat{s} = \frac{s - s_{out}(r)}{\pi r^2 \sqrt{\det \mathbf{M}}}, \quad (12)$$

since all the estimates are valid, we can pick the smallest one:

$$d \leq \min_{r>0} d(r). \quad (13)$$

Fig. 10a shows an example of the functions. A neighborhood constructed by this method is shown in Fig. 10b.

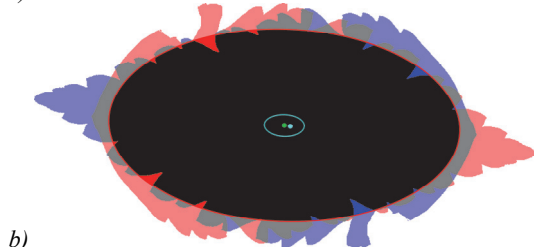
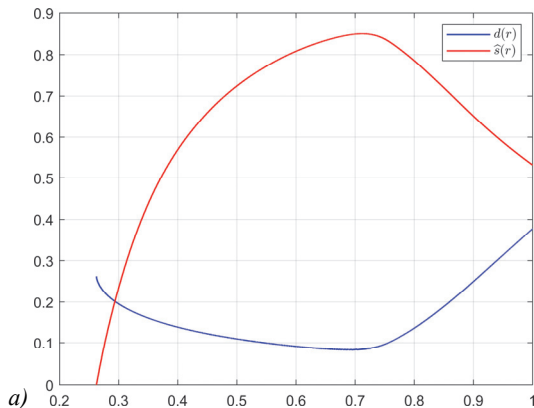


Fig. 10. a) Neighborhood size $d(r)$ and the lower estimate of the fraction of the inner area $\hat{s}(r)$ vs. the size of the approximating ellipse. The linear size of the circumscribed ellipse is assumed to be 1. b) The ellipse results in the minimum neighborhood size

It is difficult to analytically calculate the function L^{-1} inverted to $L(\hat{d})$. We proposed to use a table of values or an approximated function

$$\tilde{L}^{-1}(S) = 1.0133 - 0.5132S - 0.49845\sqrt{S}.$$

The relative error of approximation does not exceed 1.25%.

We proceeded similarly when considering higher-degree symmetries:

$$d \leq \min_{r>0} \left(r \tilde{L}^{-1} \left(\frac{\bar{s} - s_{out}(r)}{\pi r^2} \right) \right). \quad (14)$$

Note that using the center of mass and principal components to construct the approximating circles and ellipses is an intuitive heuristic. Generally, the search for an approximating figure which produces the minimum area region containing the optimal focus among all the possible circles or ellipses is still a problem to be solved.

2. Experimental search for a region containing the central (degree 2) symmetry focus

We processed 102 images from the Flavia image dataset [11] (32 images of plant leaves) and MPEG-7 CE Shape-1 Part B [12] (70 images from various categories). In all cases, the true position of focus of the rotational symmetry obtained by exhaustive search (brute force) was inside the estimated region.

Fig. 11 visualizes the size of the region calculated by (1). The region contains the rotational symmetry focus. The estimated region is shown in yellow. The true position of central symmetry focus marked as red dot.

Fig. 12 shows the detection of the region which contains the central symmetry focus. The area is inscribed in an ellipse constructed for the image.



Fig. 11. Detection of the region containing the central symmetry focus







Fig. 12. Detection of the ellipse-shaped region containing the central symmetry focus

Our key hypothesis was that the size of this region is small, so it is possible to apply a complete pixel enumeration procedure to find the true focus. To estimate the potential reduction of the enumeration space, we compared the size of the detected region in pixels with the size of the circumscribed circle and the size of a

smaller circle as proposed in [6]. Its radius was 15 % of the radius of the circumscribed circle λR , $\lambda=0.15$ (see the examples in Tab. 1). The efficiency of the region representation with an ellipse can be assessed as the ratio of the number of pixels inside the ellipse to the number of pixels inside the circle.

Tab. 1. Areas of the regions in pixels vs. the circumcircle and the number of pixels in the image

Image	Ellipse area	Circle area	Circumcircle		Figure area, pxls	Time, ms
			$\lambda = 1.0$	$\lambda = 0.15$		
	4469	6509	350116	8497	96732	28
	1756	2442	332637	10557	159809	41
	9352	19990	406717	17193	103549	32
	68	554	272638	7845	26831	12

As mentioned above, we processed more than 100 images from two datasets. The average ratio of the detected circle region to the circumcircle is 0.064. The average ratio of the detected circle region to the smaller circumcircle is 2.251. The same values for the elliptical regions are 0.055 and 1.997, respectively. The efficiency of using an ellipse instead of circle, estimated as the ratio of the corresponding areas for the entire image dataset, was 0.804.

For highly symmetric images (Jaccard index of the original and rotated figures exceeds 0.8), the size of the detected region is smaller than the arbitrary value suggested in [6]. On average, for all the images processed the value of the ratio of the areas of the found circle and the circle λR , $\lambda=0.15$ turned out to be about two. If we consider only the images with a Jaccard symmetry index greater than 0.8 (34 out of 102), the ratio is 0.084 for the ellipse approximations. It should be noted that the region detected with the empirical rule did not always contain the focus (the focus was in the region λR , $\lambda=0.15$ in 91 out of 102 cases).

In most cases, the proposed estimate gives an area significantly lower than the area with $\lambda = 0.15$. The exceptions are figures which focus of rotational symmetry does not enter the area with radius $r=\lambda R$, $\lambda=0.15$, see examples in the Tab. 2.

3. Experimental search for a region containing the rotational (degree >2) symmetry focus










Tab. 3 shows the results of comparing the proposed method and the method based on the Radon transform [8] for starfish images taken from

<https://australian.museum/learn/animals/sea-stars/sydney-seastars/> and <http://www.jaxshells.org/starfish.htm> dataset. The degree of symmetry was equal to the number of rays of the starfish. Red dots in the first row of images are rotational symmetry focuses for different angles of rotation, red dots in the bottom row are focuses averaged according to formula 7. Again, when the approximating circle covers a significant fraction of the image the size of the region detected with the methods is quite small. Being more complex, the Radon-based method is able to build regions of arbitrary, rather than only circular, shape and leaves fewer candidate points, but is much slower. At the same time, both methods successfully cope with the task and do not exclude the correct focus from consideration.

Conclusion

This study proposes an analytical, Jaccard index-based estimate of the size of a binary image region (circle or ellipse) that contains the rotational symmetry focus. The region size is the lower estimate of the intersection area as the approximating figures and taking into account the edge noise of the outline. The approximating figure is a circumscribed circle or ellipse. To verify the hypothesis that the size of the region is relatively small, we performed a simulation with image datasets. The results show that the detected regions always contained the focus, although sometimes the region size was significant. The circle region whose radius was chosen arbitrarily at 15 % of the circumcircle radius λR , $\lambda=0.15$, as suggested in [6], does not always contain the focus.

Tab. 2. Examples of some interesting cases

Image	$S_{circle}/S_{\lambda=1}$	$S_{circle}/S_{\lambda=0.15}$	$S_{ellipse}/S_{\lambda=1}$	$S_{ellipse}/S_{\lambda=0.15}$	$S_{ellipse}/S_{circle}$	The focus is inside the area with $\lambda=0.15$	Time, ms
	0.009	0.343	0.007	0.248	0.724	+	41
	0.221	7.929	0.341	12.254	1.545	-	11
	0.387	8.596	0.482	10.707	1.246	-	15
	0.243	11.059	0.251	11.393	1.030	-	19
	0.037	1.257	0.001	0.045	0.036	+	11
	0.037	1.387	0.006	0.217	0.158	+	20
	0.013	0.586	0.005	0.217	0.372	+	16
	0.009	0.343	0.007	0.248	0.724	+	9
	0.127	5.626	0.428	18.989	3.375	-	4

This study proposes an analytical, Jaccard index-based estimate of the size of a binary image region (circle or ellipse) that contains the rotational symmetry focus. The region size is the lower estimate of the intersection area as the approximating figures and taking into account the edge noise of the outline. The approximating figure is a circumscribed circle or ellipse. To verify the hypothesis that the size of the region is relatively small, we performed a simulation with image datasets. The results show that the detected regions always contained the focus, although sometimes the region size was significant. The circle region whose radius was chosen arbitrarily at 15% of the circumscribed radius λR , $\lambda=0.15$, as suggested in [6], does not always contain the focus.

References

- [1] Lei Y, Wong KC. Detection and localization of reflectional and rotational symmetry under weak perspective projection. *Pattern Recogn* 1999; 32(2): 167-180.
- [2] Yip RKK. Genetic Fourier descriptor for the detection of rotational symmetry. *Image Vis Comput* 2007; 25: 148-154.
- [3] Yip RK, Lam WC, Tam PK, Leung DN. A Hough transform technique for the detection of rotational symmetry. *Pattern Recogn Lett* 1994; 15(9): 919-928.
- [4] Lladós J, Bunke H, Martí E. Finding rotational symmetries by cyclic string matching. *Pattern Recogn Lett* 1997; 18(14): 1435-1442.
- [5] Aguilar W, et al. Detection of rotational symmetry in curves represented by the slope chain code. *Pattern Recogn* 2020; 107: 107421.
- [6] Seredin O, Liakhov D, Kushnir O, Lomov N. Jaccard index-based detection of order 2 rotational quasi-symmetry

focus for binary images. Pattern Recogn Image Anal 2022; 32(3): 672-681.

[7] Jaccard P. Étude comparative de la distribution florale dans une portion des Alpes et des Jura. Bull Soc Vaudoise Sci Nat 101; 37: 547-579.

[8] Lomov N, Seredin O, Kushnir O, Liakhov D. Search for rotational symmetry of binary images via radon transform and fourier analysis. Proc 18th Int Joint Conf on Computer Vision, Imaging and Computer Graphics Theory and Applications (VISAPP) 2023; 4: 280-289.



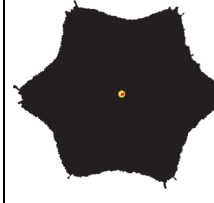
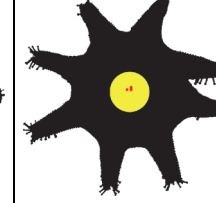
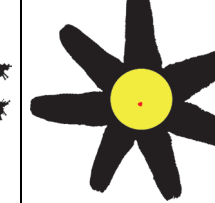
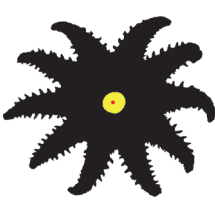

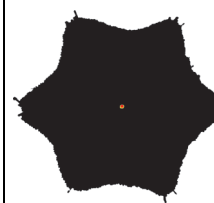
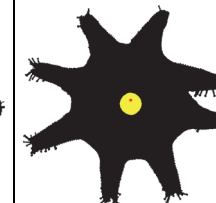
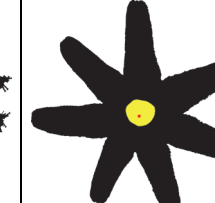
[9] Dimitrov D, Knauer C, Kriegel K, Rote G. Bounds on the quality of the PCA bounding boxes. Comput Geom 2009; 42(4): 772-789. DOI: 10.1016/j.comgeo.2008.02.007.

[10] Shiang S-P, Liu J-S, Chien Y-R. Estimate of minimum distance between convex polyhedra based on enclosed ellipsoids. IEEE Int Conf on Intelligent Robots and Systems 2000; 1: 739-744. DOI: 10.1109/IROS.2000.894692.

[11] Wu SG, Bao FS, Xu EY, Wang Y-X, Chang Y-F, Xiang Q-L. A leaf recognition algorithm for plant classification using probabilistic neural network. 2007 IEEE Int Symposium on Signal Processing and Information Technology 2007: 11-16.

[12] Latecki LJ, Lakamper R. Shape similarity measure based on correspondence of visual parts. IEEE Trans Pattern Anal Mach Intell 2000; 22(10): 1185-1190.

Tab. 3. Detection of the region containing higher order rotational symmetry focuses for different angles of rotation

Image Size	555×469	482×463	1095×989	1105×1048	1343×1359
Result (Proposed method)					
Region area (proposed)	12204	9191	971	33493	117722
Time, ms (proposed)	38	23	270	191	286
Result (Radon transform-based method)					
Region Area (Radon)	2571	1944	344	9782	23749
Time, ms (Radon)	121	38	169	302	590

Authors' information

Nikita Aleksandrovich Lomov was born in 1992. In 2015 graduated from Lomonosov Moscow State University as a specialist in Applied Mathematics and Computer Science. In 2020 defended the Ph.D. thesis on "Morphological descriptors of variable-width objects in digital images". He is now a senior research scientist in Tula State University. Nikita Lomov is an investigator of several grants of the Russian Science Foundation, Russian Fund for Basic Research and the Ministry of Education and Science of Russian Federation. Research interests: computer vision, image processing, computational geometry, shape analysis, medial representations. He is the author of more than 20 scientific papers and a number of applied software packages. E-mail: nikita-lomov@mail.ru.

Oleg Sergeevich Seredin holds a Ph.D. in Theoretical Foundations of Computer Science from the Computing Center of the Russian Academy of Sciences in Moscow, with his thesis on Methods and Algorithms of Featureless Pattern Recognition completed in 2001. Currently, he is an Associate Professor at the School of Applied Mathematics and Computer Science, Tula State University (TSU), and is a Leading Researcher at the Laboratory of Cognitive Technologies and Simulating Systems, TSU. His research interests include data mining, pattern recognition, machine learning, signal and image analysis, visual representation of multidimensional data, and statistical methods for decision making. Prof. Seredin has served on the program committee of many conferences, including CloudCom, AIST, GraphiCon, VISAPP, PSBB, PRIB, and MaDaIn. He is also a member of the reviewer board for several journals, such as Sensors, Computer Optics, SN Computer Science Journal, IEEE Signal Processing Letters, and Applied Science. He has been the

supervisor of several research projects funded by the grants from the Russian Science Foundation and the Russian Fund for Basic Research, and international grants. He has worked as a visiting researcher at Rutgers University and National Taipei University of Technology. Prof. Seredin has authored more than 100 scientific papers in refereed journals and conference proceedings on machine learning, pattern recognition, and computer vision. He is a member of the International Association for Pattern Recognition (IAPR). E-mail: oseredin@yandex.ru.

Daniil Viktorovich Liakhov is a student of Tula State University, specialty of Informational Systems and Technologies and assistant-researcher at the Laboratory of Cognitive Technologies and Simulating Systems of Tula State University. Now he is involved as researcher to the grant project of Russian Science Foundation. E-mail: liakhov.daniil@mail.ru.

Olesia Aleksandrovna Kushnir received the Ph.D. Degree in Engineering and Technologies from Tula State University. Ph.D. Thesis: “Methods and algorithms for binary images matching based on skeletonization” (2018). Now she is an Associate Professor at the School of Applied Mathematics and Computer Science, Tula State University (TSU), and is a Senior Researcher at the Laboratory of Cognitive Technologies and Simulating Systems, TSU. Her scientific interests are signal and image analysis, shape analysis, data mining, pattern recognition, machine learning. Olesia Kushnir was principal investigator of a grant of the Russian Fund for Basic Research, and takes part in grants of other researchers. She worked as visiting scientist at Institute of Computer Vision and applied Computer Sciences (IBaI), Leipzig, Germany, and National Taipei University of Technology. She was a student in International Computer Vision Summer School (ICVSS), Sicily, Italy. She has published more than 40 scientific papers in refereed journals, hand-books, and conference proceedings in the areas of computer vision, machine learning, pattern recognition. E-mail: kushnir-olesya@rambler.ru.

*Code of State Categories Scientific and Technical Information (in Russian – GRNTI): 28.23.15.
Received May 24, 2023. The final version – June 22, 2023.*
